

Photoluminescence of Si-rich Si-Ge alloys

G. S. Mitchard and T. C. McGill

California Institute of Technology, Pasadena, California 91125

(Received 27 July 1981)

A detailed study of the photoluminescence spectrum of $\text{Si}_{1-x}\text{Ge}_x$ is presented for $x \approx 0.1$. Undoped and In-doped alloy samples are investigated. Spectral features are identified, and the effects of the disordered nature of the alloy on the luminescence spectrum are discussed. In particular, mechanisms for the observed broadening of bound-exciton luminescence are discussed, and the shift in alloy luminescence energy is obtained. At low temperatures a luminescence feature is observed which may result from recombination of excitons bound to local fluctuations in alloy composition.

I. INTRODUCTION

The properties of alloy semiconductors have been of general interest for some time. Such alloys provide a convenient system with which to experimentally and theoretically study the effects of disorder, which can be varied with alloy composition. The band gap can also be varied with alloy composition, and for this reason considerable effort has been directed towards the development of intrinsic and extrinsic alloy optoelectronic devices. The study of the luminescence properties of alloy semiconductors can provide useful and relatively easily interpreted information regarding the properties of the alloys and the consequences of their disordered nature. Most attention has been directed towards the III-V ternary alloys, where luminescence processes have been studied extensively.¹⁻³ Luminescence of II-VI ternary alloys has also been studied, most notably $\text{Hg}_{1-x}\text{Cd}_x\text{Te}$ (Ref. 4) where ir detector applications are particularly important.

Another alloy material of interest is the binary alloy $\text{Si}_{1-x}\text{Ge}_x$. The luminescence properties of $\text{Si}_{1-x}\text{Ge}_x$ are not particularly well known, although free- and bound-exciton,⁵ donor-acceptor,⁶ and electron-hole droplet⁷ recombination has been observed in Ge-rich alloys. In this paper we report the first detailed measurements of luminescence from Si-rich alloys, in particular alloys for which $x \approx 0.1$. Intrinsic and impurity-related luminescence is discussed, as well as certain properties of the luminescence which arise as a result of the compositional disorder of the alloy. In particular, we have been able to identify the luminescence features which result from free-exciton and bound-exciton recombination in the alloy. Also,

mechanisms for the observed bound-exciton luminescence broadening are discussed. Comparison of the luminescence energies from Si and the alloy samples results in values for the band-gap shift and free-exciton binding energy for the values of the composition parameter x which we were able to study. Finally, some evidence is presented which suggests that we observe at low temperatures luminescence which is the result of recombination of excitons bound to local fluctuations in alloy composition.

The remainder of this paper is organized in the following way. In Sec. II, we discuss the $\text{Si}_{1-x}\text{Ge}_x$ alloy samples studied, and the general features of the experimental technique. In Sec. III, the results of measurements on the undoped $\text{Si}_{1-x}\text{Ge}_x$ samples are presented and discussed. In Sec. IV, we consider the results obtained for one In-doped $\text{Si}_{1-x}\text{Ge}_x$ sample. In Sec. V, we discuss the general mechanisms for luminescence line broadening in the alloy, compare the alloy luminescence energies with those observed in Si, and consider the evidence for excitons bound to composition fluctuations. Finally, in Sec. VI, the results are summarized.

II. EXPERIMENTAL CONSIDERATIONS

A. Si-Ge alloy samples

In this paper, we present measurements of the photoluminescence properties of three $\text{Si}_{1-x}\text{Ge}_x$ samples, two of which were not intentionally doped and the third of which was doped with In. The crystals were grown by the Czochralski technique.

Impurity concentrations and alloy compositions were determined at Hughes Research Laboratories, where the crystals were grown. Impurity concentrations were established on the basis of Hall-effect measurements. These measurements show that residual concentrations of B and P impurities are present in all the samples. Alloy compositions were obtained from a variety of techniques; results of the electron microprobe, density, and x-ray diffraction measurements were in excellent agreement. The samples studied, their impurity concentrations, and their alloy compositions are given in Table I.

B. Experimental technique

The Si-Ge alloy samples described above were mechanically etched, and then mounted in a Janis variable-temperature cryostat. The luminescence resulted from above band-gap optical excitation by a Spectra-Physics Model 166 Ar⁺ laser, which could be operated in pulsed or cw mode. The luminescence was collected from the edge of the sample, wavelength-analyzed with a Spex Model 1269 spectrometer, and detected with an RCA 7102 S-1 photomultiplier cooled to liquid-nitrogen temperature. The photomultiplier output was processed with standard photon-counting electronics, acquired on a Nuclear Data ND-60 multichannel analyzer, and finally passed to a PDP 11/34 computer for analysis and storage.

III. EXPERIMENTAL RESULTS AND DISCUSSION FOR UNDOPED Si_{1-x}Ge_x

In this section, the results of the application of the photoluminescence technique to the undoped samples are considered. Two undoped Si_{1-x}Ge_x samples were available, C077 ($x=0.11$) and C021-3 ($x=0.067$). As indicated in Table I, these samples

have low residual concentrations of B and P impurities, in spite of not being intentionally doped.

A. Typical photoluminescence spectrum and identification of phonon replicas

A typical low-temperature photoluminescence spectrum of sample C077 is shown in Fig. 1. Two broad features are visible at the high-energy end of the spectrum and are labeled FE (free exciton) and BE_P (bound exciton). Replicas of these lines, labeled FE(TO) and BE_P(TO), are observed approximately 58 meV lower in energy. Since this is the transverse-optical (TO) phonon energy in Si, the low-energy lines are interpreted as being due to TO phonon replicas of the higher-energy lines.

B. Identification of free-exciton luminescence

In this section we consider the effect of increasing the sample temperature on the photoluminescence spectrum of sample C077. In Fig. 2 we see that as the temperature is increased the line labeled BE_P thermalizes with respect to the line labeled FE. Above 10 K (Fig. 3), the line labeled BE_P is no longer visible, and the line labeled FE assumes a shape characteristic of free-exciton (FE) recombination in Si. In intrinsic Si, FE recombination luminescence has been fitted very accurately with a line shape,⁸

$$I(E) \propto \sqrt{E-E_0} \exp \left[\frac{E-E_0}{k_B T} \right], \quad (1)$$

where $I(E)$ is the luminescence intensity at photon energy E , E_0 is the FE threshold energy, and T is the temperature. In this expression we assume parabolic FE bands and a Boltzmann distribution of FE center-of-mass kinetic energies. The high-temperature luminescence from sample C077 can

TABLE I. Si_{1-x}Ge_x alloys studied using photoluminescence. The samples were grown and characterized at Hughes Research Laboratories.

Sample	N_B (cm ⁻³)	N_P (cm ⁻³)	x		Electron microprobe	Density	X-ray diffraction
			N_{In} (cm ⁻³)				
C077	3.6×10^{13}	2.8×10^{13}			0.1115	0.113	0.113
C021-3	2.3×10^{14}	4.1×10^{14}			0.0677	0.0685	
C093	5.0×10^{15}	5.3×10^{14}	2.5×10^{16}				0.104

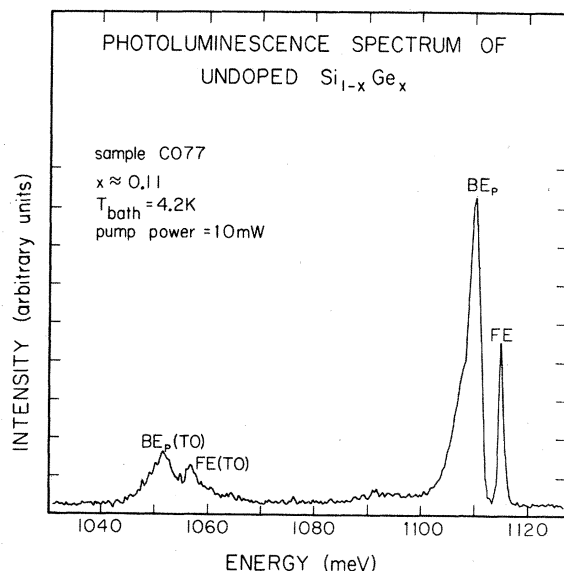


FIG. 1. Typical photoluminescence spectrum of undoped $\text{Si}_{1-x}\text{Ge}_x$ sample C077. Refer to the text for an explanation of the line assignments.

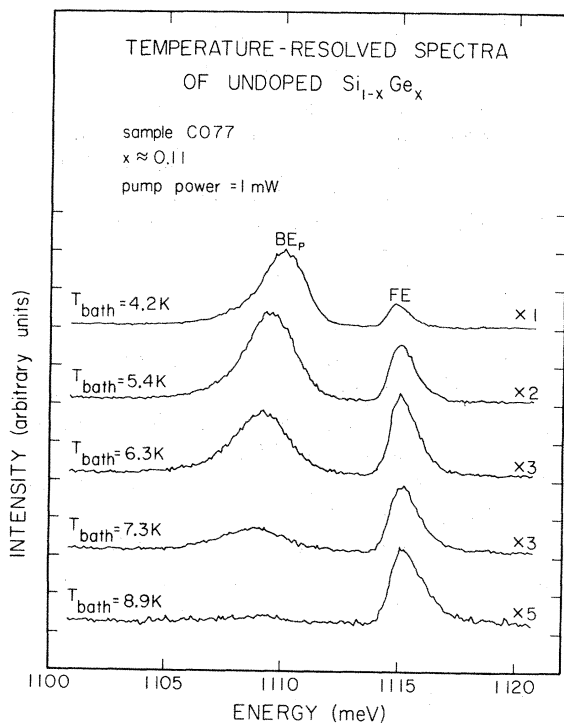


FIG. 2. Temperature-resolved spectra of undoped $\text{Si}_{1-x}\text{Ge}_x$ sample C077 from 4.2 to 8.9 K. The scale factors (e.g., $\times 2$) give the relative intensity magnification. Note that thermalization of the line labeled BE_p is observed. In addition, the BE_p peak position shifts to lower energy as the temperature is increased. At high temperatures, the luminescence of the line labeled FE assumes a shape characteristic of free-exciton luminescence in Si.

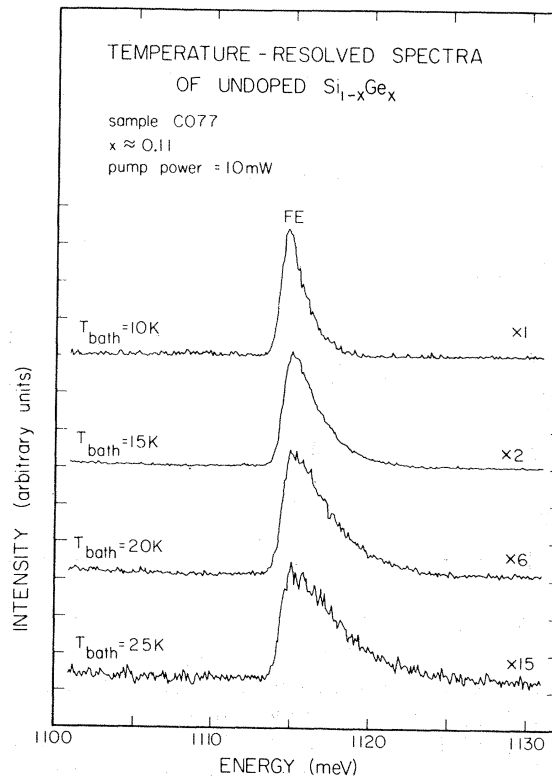


FIG. 3. Temperature-resolved spectra of undoped $\text{Si}_{1-x}\text{Ge}_x$ sample C077 from 10 to 25 K. The scale factors (e.g., $\times 2$) give the relative intensity magnification. Note that, at these temperatures, the luminescence of the line labeled FE assumes a shape characteristic of free-exciton luminescence in Si.

also be fitted very well with the line shape described by Eq. (1). An example of this fit is shown in Fig. 4. In all cases, the fit temperature obtained in this manner was within 1 K of the measured bath temperature. Also, the threshold energy remained constant within 0.05 meV. On the basis of this analysis, the line labeled FE is identified as resulting from no-phonon (NP) FE recombination. Note that this intrinsic NP luminescence is greatly enhanced in the alloy, since the Ge atoms can act as momentum-conserving scattering centers.⁵

C. Identification of bound-exciton luminescence

The identification of the FE line obtained in the preceding section, splitting between the FE threshold and the peak position of the line labeled BE_p , and the thermal behavior shown in Fig. 2, suggest that the line labeled BE_p is due to the NP recom-

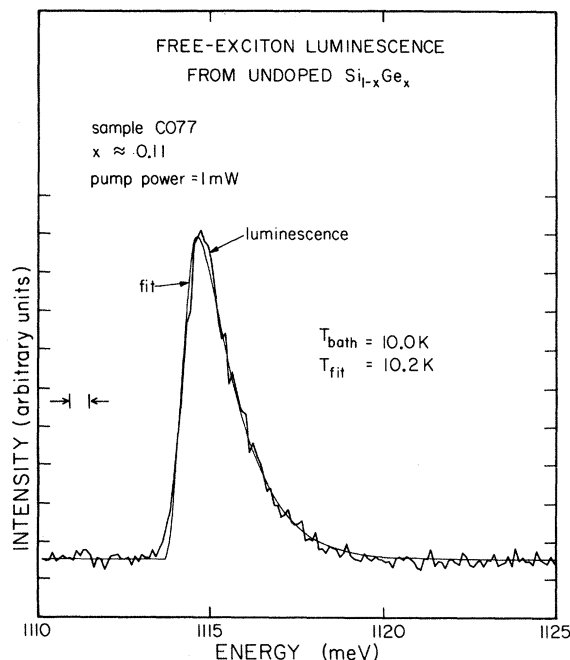


FIG. 4. Free-exciton luminescence from undoped $\text{Si}_{1-x}\text{Ge}_x$ sample C077 and least-squares fit of the theoretical line shape [Eq. (1)]. The sample temperature obtained as a result of the fit T_{fit} is shown with the measured bath temperature T_{bath} .

bination of excitons bound by about 4 meV to a shallow level. The pump-power dependence at low power shown in Fig. 5 supports this proposal. As this figure demonstrates, the FE to BE_p luminescence intensity ratio is independent of pump power.

Candidates for such a level are clearly B and P, which have binding energies in the neighborhood of 4 meV in Si (3.9 and 4.7 meV, respectively⁸), and which are the most common shallow impurities in the undoped material. Photoluminescence measurements of Si containing approximately equal background concentrations of B and P show that P bound-exciton (BE_p) luminescence is more intense than B bound-exciton (BE_B) luminescence in the NP region by at least an order of magnitude. It seems reasonable to conclude, therefore, that the line labeled BE in the luminescence from sample C077 is primarily due to NP BE_p recombination.

The high-power pump-power dependence presented in Fig. 6 supports this conclusion. In undoped Si, low-energy lines due to bound-multiexciton complexes (BMEC) appear as the pump power is increased. The splitting between the BE_p line and the first BMEC line is 2.2 meV for B and 3.6 meV for P.⁹ As shown in Fig. 6, in the luminescence spectrum of sample C077 the

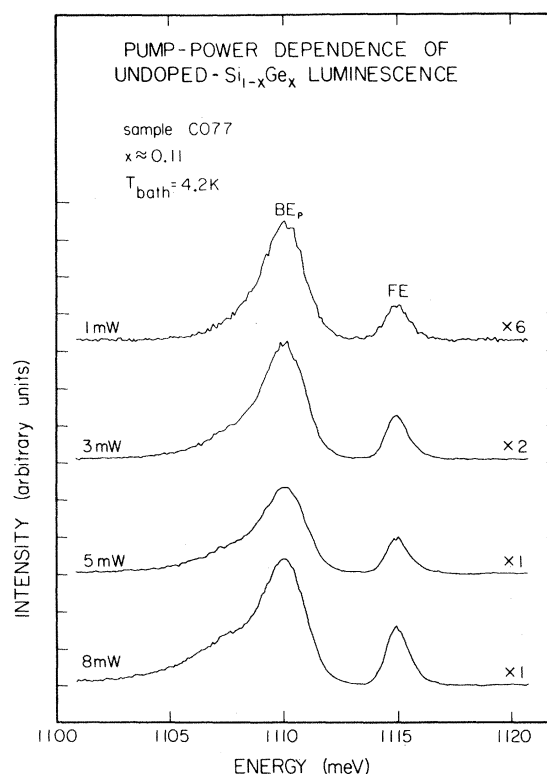


FIG. 5. Pump-power dependence of the luminescence from undoped $\text{Si}_{1-x}\text{Ge}_x$ sample C077 at low pump powers. The scale factors (e.g., $\times 6$) give the relative intensity magnification. Note that the BE_p to FE luminescence intensity ratio is independent of pump power at these power levels.

BE_p line develops a low-energy shoulder as the pump power is increased, which resolves into a separate line at high pump powers. The separation between this line and the BE_p line is about 3.8 meV, which is consistent with the splitting between the P BE and first BMEC in Si. Since no line is observed which would correspond to B BMEC luminescence, our conclusion regarding the origin of the BE_p line in the alloy seems justified.

D. Comparison of photoluminescence spectra

The interpretation of the photoluminescence spectrum of sample C077 developed in the previous sections is consistent with our investigation of the $x = 0.067$ sample, C021-3. In Fig. 7, the luminescence spectra of samples C077 and C021-3 are compared. We see that the ratio of BE_p to FE luminescence is considerably greater for sample C021-3. This is consistent with Table I, which in-

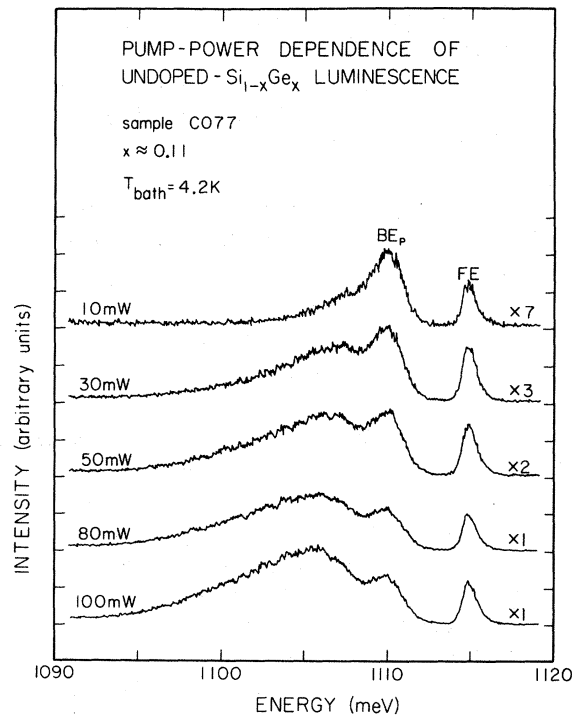


FIG. 6. Pump-power dependence of luminescence from undoped $\text{Si}_{1-x}\text{Ge}_x$ sample C077 at high pump powers. The scale factors (e.g., $\times 7$) give the relative intensity magnification. Note the new feature which appears on the low-energy side of the BE_p line at high pump powers. This feature is discussed in the text.

dicates that impurity concentrations in sample C021-3 are approximately an order of magnitude higher. In addition, we see that the luminescence spectrum of sample C021-3 is shifted to higher energy. This feature will be discussed in detail below.

IV. EXPERIMENTAL RESULTS AND DISCUSSION FOR In-DOPED $\text{Si}_{1-x}\text{Ge}_x$

The subject of the investigations reported in this section was the In-doped $\text{Si}_{1-x}\text{Ge}_x$ sample C093, for which $x = 0.10$.

A. Typical photoluminescence spectra

Typical luminescence spectra obtained from $\text{Si}_{1-x}\text{Ge}_x$: In sample C093 are shown in Fig. 8. Spectra measured at various temperatures are shown. Two features are prominent in the spectra. The higher-energy luminescence, labeled FE, be-

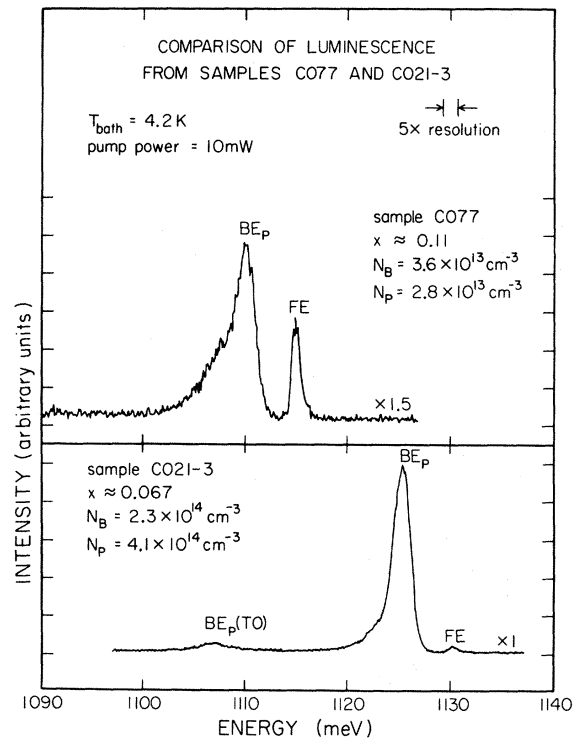


FIG. 7. Comparison of the luminescence spectra of samples C077 and C021-3. The scale factors (e.g., $\times 1.5$) give the relative intensity magnification. Note that BE_p luminescence is much more intense from sample C021-3 than from sample C077. Also, note that the luminescence from sample C021-3 is at higher energy than the luminescence from sample C077. These features are discussed in the text.

comes visible only at high temperatures. At somewhat lower energies a broad feature labeled L is visible, which moves to lower energy as the temperature is increased. The L luminescence develops a low-energy shoulder at high temperatures, which has been labeled $\text{FE}(\text{TO})$.

B. Identification of free-exciton luminescence

To begin with, we note that the luminescence labeled FE has a line shape and temperature dependence characteristic of NP FE recombination in Si, as described in detail in Sec. III. Equation (1), which describes the NP FE line shapes, can be fitted to the FE luminescence from sample C093 very accurately. The FE threshold energy obtained from such fits, 1115.8 meV, remained constant within about 0.3 meV. However, the fit temperatures T_{fit} were systematically higher than the mea-

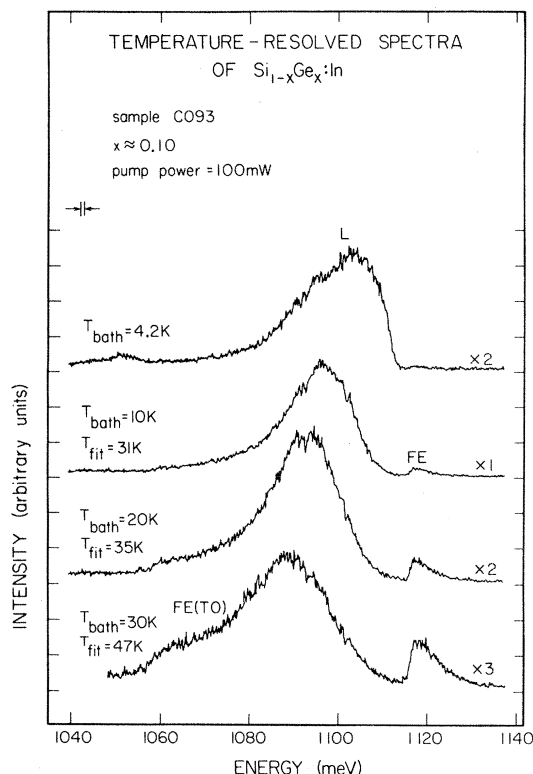


FIG. 8. Temperature-resolved spectra of $\text{Si}_{1-x}\text{Ge}_x\text{:In}$ sample C093 from 4.2 to 30 K. The scale factors (e.g., $\times 2$) give the relative intensity magnification. Refer to the text for a discussion of the line assignments shown in the figure. Where FE luminescence is observed, the sample temperature obtained from a least-squares fit to the FE line shape, T_{fit} , is shown with the measured bath temperature T_{bath} . The discrepancy between these results is discussed in the text.

sured bath temperatures T_{bath} . These temperatures are indicated in Fig. 8. It seems, therefore, that either the FE luminescence is subject to some broadening as a result of the disordered nature of the alloy, or the sample is being locally heated by the laser pump. Of these two possibilities, the second seems most likely. First, one would expect some broadening mechanism to affect the FE threshold behavior as well as generally broaden the line. That is, we would expect to see the FE threshold "smear out" and become less abrupt. However, this behavior is not observed. As previously mentioned, the line shape is described by Eq. (1) very well. Second, as indicated in Table I sample C093 has impurity concentrations which are about 3 orders of magnitude higher than those in sample C077. As a result, much higher pump powers are needed to observe FE luminescence at all in sample C093. At these laser intensities, sam-

ple heating must be considered a very likely cause of the observed FE broadening.

If this explanation is accepted, the luminescence labeled FE can be interpreted as resulting from NP-FE recombination in the $\text{Si}_{1-x}\text{Ge}_x\text{:In}$ alloy. Since the feature labeled FE(TO) is separated from the FE peak by approximately the Si TO phonon energy, we interpret this shoulder on L as being due to TO phonon-assisted FE recombination.

C. Identification of bound-exciton luminescence

Our interpretation of the luminescence labeled L is necessarily considerably more complicated than that of the FE luminescence. There are a number of processes which are undoubtedly contributing to the L line. Primarily, BE_B , BE_P , and BE_{In} luminescence must be considered. Indium, of course, is the majority dopant, and will dominate the NP-BE luminescence. The B concentration is about an order of magnitude greater than the P concentration. It follows from our discussion of BE luminescence from undoped $\text{Si}_{1-x}\text{Ge}_x$ that B and P will probably contribute equally to the NP-BE luminescence. In addition, the L luminescence is sufficiently broad that transverse-acoustic (TA) phonon replicas of the FE and BE lines may contribute as well. It is unlikely that NP-BMEC or electron-hole-droplet (EHD) luminescence will have any significant influence on the spectra presented here. The impurity concentrations in sample C093 preclude the observation of such effects at the pump powers utilized in this study.

1. Time-resolved spectra and isolation of B bound-exciton component

In an effort to separate the BE components which produce the L luminescence, the time evolution of the luminescence from sample C093 was measured at low pump power. The time-resolved spectra are shown in Fig. 9 for low-power laser excitation. As this figure demonstrates, the L luminescence is composed of a relatively sharp high-energy component with a long lifetime, and a broad low-energy component with a short lifetime. Consideration of the BE_B , BE_P and BE_{In} decay times in Si (1055, 272, and 2.7 nsec, respectively¹⁰) leads to the suggestion that the sharp, long-lifetime component is primarily a result of BE_B recombination. The broad, short-lifetime, low-energy shoulder is therefore probably due to BE_{In} recombination.

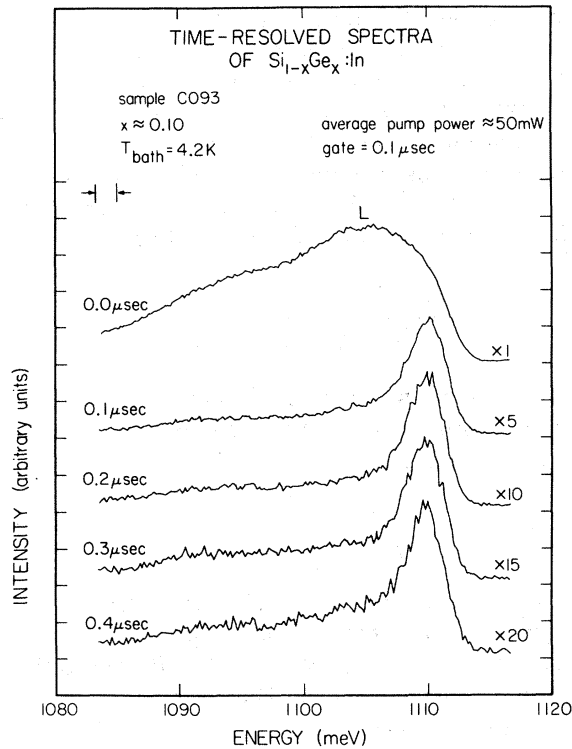


FIG. 9. Time-resolved spectra of $\text{Si}_{1-x}\text{Ge}_x\text{In}$ sample C093. The scale factors (e.g., $\times 5$) give the relative intensity magnification. At long times, a sharp, long-lifetime component of L luminescence is isolated.

2. Temperature-resolved spectra and isolation of In bound-exciton component

A further separation of the BE components which produce the L luminescence can be accomplished by measuring the temperature dependence of the photoluminescence spectrum. This measurement is shown in Fig. 8. We see that the high-energy side of the L luminescence thermalizes as the temperature is increased. This observation is consistent with the interpretation of L luminescence presented in the previous section. At high temperatures, only the lower-energy BE_{In} component is observed. The higher-energy BE_{B} component has thermalized.

This effect is seen clearly in Fig. 10, which shows the temperature dependence of L luminescence which is gated in time. At low temperatures, the BE_{B} peak is reasonably well isolated. At the high pump powers used for this measurement, however, a low-energy shoulder is clearly observed. We interpret this shoulder as being due to a BE_{In} component which has not been eliminated by the time resolution. As the temperature is increased,

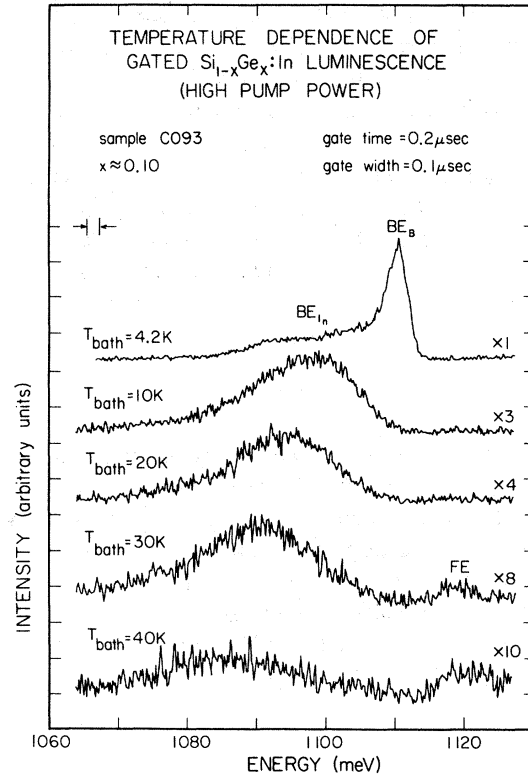


FIG. 10. Gated, temperature-resolved spectra of $\text{Si}_{1-x}\text{Ge}_x\text{In}$ sample C093 at high pump power. The scale factors (e.g., $\times 3$) give the relative intensity magnification. At high temperature, the BE_{B} luminescence component thermalizes, and the BE_{In} component is isolated. At high temperatures, weak FE luminescence is also observed.

we see the BE_{B} component thermalize with respect to the BE_{In} component. Above 10 K, only the BE_{In} component remains.

There is one difficulty with this interpretation which should be mentioned. As the temperature is raised above 10 K, the BE_{In} component peak position moves to lower energy, as expected from the behavior of BE_{P} luminescence in undoped $\text{Si}_{1-x}\text{Ge}_x$. This effect is observed in Fig. 8 and Fig. 10. However, the BE_{In} peak moves too far; at 30 K, it is already approximately 25 meV below the FE threshold, while the BE_{In} binding energy in Si is only 13.7 meV.¹¹ In spite of this, the bulk of the experimental evidence supports the interpretation that this high-temperature luminescence is due to BE_{In} recombination in the alloy. It may be that contributions from FE and BE TA-assisted luminescence combine to produce the anomalously low high-temperature BE_{In} peak position. However, this seems unlikely when the relative intensities of TA and NP luminescence in Si are considered.

It is also possible that the high-temperature BE_{In} binding energy in the alloy is increased as a result of some complicated effect which may involve the unusually large radii of the Ge and In atoms relative to the Si—Si bond length. Of course, this mechanism is also unlikely, practically by definition. Unfortunately, all we can state at this point is that the anomalous temperature dependence of the BE_{In} luminescence remains unexplained.

V. DISCUSSION

In the previous sections, we have presented the experimental photoluminescence data for the undoped and In-doped Si-Ge alloy samples, and have attempted to interpret the spectra qualitatively. In this section, we continue our qualitative discussion of the experimental results. In particular, we focus on some effects which result from the compositional disorder of the alloy.

A. Bound-exciton line broadening

To begin with, we see that the BE line is considerably broadened in the alloy. In fact, the BE line in the undoped $Si_{1-x}Ge_x$ samples is approximately ten times broader (~ 3 meV) than its counterpart in Si (~ 0.4 meV). In general, this broadening can be accounted for on the basis of the compositional inhomogeneity of the alloy material. The energy of the luminescence which results from the recombination of an exciton bound to a particular impurity will depend on the local configuration of Si and Ge atoms. This luminescence energy can be schematically written as

$$E_{PL}(\{c\}) = E_G(\{c\}) - E_{FE}(\{c\}) - E_{BE}(\{c\}), \quad (2)$$

where E_{PL} is the photon energy, E_G is the band-gap energy, E_{FE} is the free-exciton binding energy, and E_{BE} is the bound-exciton binding energy, and where $\{c\}$ denotes the particular configuration for the impurity being considered.

We can consider two simple limits to the general expression, Eq. (2). First, we assume that the local configuration does not affect the free-exciton binding energy or bound-exciton binding energy. Then Eq. (2) indicates that the BE-line broadening is the result of variations in band-gap energy produced by local fluctuations in the alloy composition x . This limit was first discussed by Alferov *et al.*¹²

We can roughly estimate this effect on the basis of the following argument. Given a volume $4\pi a^3/3$, there will be $4\pi a^3 \propto N/3$ atoms, where N is the density of lattice sites in the alloy, if the Ge atoms are distributed randomly the typical fluctuation in the number of Ge atoms in the volume will be $(4/3\pi a^3 x N)^{1/2}$. Therefore, the typical fluctuation in the composition parameter x will be

$$\Delta x \sim \frac{(\frac{4}{3}\pi a^3 x N)^{1/2}}{\frac{4}{3}\pi a^3 N} = \left[\frac{x}{\frac{4}{3}\pi a^3 N} \right]^{1/2}. \quad (3)$$

If $\Delta E = \alpha \Delta x$, where ΔE is the change in gap energy produced by a change in composition Δx , then Eq. (3) becomes

$$\Delta E \sim \alpha \left[\frac{x}{\frac{4}{3}\pi a^3 N} \right]^{1/2}. \quad (4)$$

N can be estimated for the alloy from the lattice-constant measurements of Dismukes *et al.*¹³ For $x=0.1$, we find $N \sim 6 \times 10^{21} \text{ cm}^{-3}$. From the absorption measurements of Braunstein *et al.*,¹⁴ we can estimate $\alpha \sim 600$ meV. Assuming that a is approximately an exciton Bohr radius in Si, i.e., about 40 Å, we obtain $\Delta E \sim 5$ meV, which is reasonable agreement for a crude calculation.

In spite of the agreement, this limit does not explain the temperature-dependence data presented in Figs. 2 and 8. The data clearly shows that the BE peak shifts to lower energy as the temperature increases. However, the band-gap fluctuation limit does not produce this behavior. In this limit, we expect that as the temperature increases excitons will thermalize to bound-exciton states in the regions where the band gap is larger, which produces a BE peak which moves to higher energy.

The second limit to Eq. (2) we will consider accounts for the observed temperature dependence. In this limit, we assume that the local configuration does not affect the band-gap energy or the FE binding energy. We assume that the gap energy and the FE binding energy are the bulk average values for the alloy. Then the BE line broadening is the result of variations in the BE binding energy caused by variations in the local configuration of Si and Ge atoms. It is possible, therefore, that the BE line is composed of several overlapping luminescence lines from BE's with slightly different binding energies. These binding energies will increase, in principle, from the BE binding energy in Ge to the BE binding energy in Si.

Qualitatively, this limit produces the temperature dependence observed in Figs. 2 and 8. At low

temperatures, we see luminescence from all BE's. As the temperature increases, though, we expect that luminescence from the most tightly bound BE's will dominate. As we have previously mentioned, these BE's will have the most Si-like local configuration. In addition to explaining the temperature-dependence data, this picture of BE-line broadening is consistent with time-resolved spectra of the alloy luminescence. An analysis of the relevant decay times shows that the decay of all components of BE luminescence is capture-limited in the cases studied here.¹⁵ This is consistent with our observation that all components of the BE line decay at the same rate — the line shape does not change and the peak position remains fixed.

B. Comparison of Si and Si-Ge luminescence energies

If we assume that, at high temperatures, the BE luminescence is dominated by components which have the most Si-like local configuration, then a procedure for directly comparing Si and $\text{Si}_{1-x}\text{Ge}_x$ luminescence energies presents itself. We propose that the difference in recombination energy between the high-temperature BE-peak position in the Si-Ge alloy and the corresponding BE-peak position in Si is just due to the shift in band gap of the alloy.

Figure 11 schematically illustrates the consequences of this proposal for the $x=0.11$ $\text{Si}_{1-x}\text{Ge}_x$ sample, C077. The high-temperature BE_p luminescence line position, 1108.71 meV, was obtained from the 8.0-K spectrum. This was the highest temperature at which BE_p luminescence could be reliably observed, and it was assumed that the luminescence was dominated by recombination of BE_p 's in essentially a Si environment. The P luminescence line position in Si, 1150.11 meV, was obtained from direct measurement of lightly doped Si:P. If this change in line position is attributed solely to a change in gap energy, these measurements imply a band-gap decrease of 41.4 meV for $x=0.11$. This value fluctuated by about 0.6 meV due to large-scale inhomogeneities in the crystals being examined. If a rough graphical extrapolation of the absorption data published by Braunstein *et al.*¹⁴ is attempted, we obtain an alloy band-gap shift of approximately 60 meV for $x=0.11$, which is in reasonable agreement with the luminescence data.

SCHEMATIC COMPARISON OF UNDOPED-Si AND UNDOPED- $\text{Si}_{1-x}\text{Ge}_x$ LUMINESCENCE ENERGIES

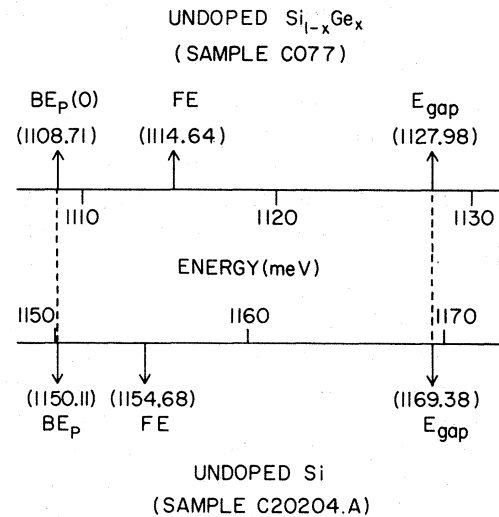


FIG. 11. Schematic line-position comparison between Si and $\text{Si}_{1-x}\text{Ge}_x$ sample C077. This comparison is based on the assumption that the difference between the energy of high-temperature BE_p alloy luminescence is equal to the difference in band-gap energies for Si and $\text{Si}_{1-x}\text{Ge}_x$ sample C077. This fixes the alloy gap energy. The spectra are then compared by lining up the Si and $\text{Si}_{1-x}\text{Ge}_x$ gap energies.

In addition to the high-temperature $\text{Si}_{1-x}\text{Ge}_x$ BE_p line position and the Si BE_p line position, Fig. 11 also shows the FE threshold and E_{gap} positions for Si and the $x=0.11$ alloy. The FE threshold position in the alloy, 1114.64 meV, was obtained by fitting Eq. (1) to the high-temperature FE luminescence spectra (Fig. 3), as illustrated in Fig. 4. The NP-FE threshold position in Si, 1154.68 meV, was obtained by fitting Eq. (1) directly to NP-FE luminescence from pure Si. The Si gap energy, 1169.38 meV, was determined from the NP-FE threshold energy by adding the FE binding energy, which is 14.7 meV. Then the alloy gap energy, 1127.98 meV, was obtained by subtracting the band-gap shift, 41.4 meV, from the Si gap energy.

As indicated in Fig. 11, this method implies that the FE dissociation energy in the $x=0.11$ alloy has decreased by 1.36 meV from its value in Si, to 13.34 meV. This compares favorably with a rough estimate based on a linear interpolation between the FE dissociation energies in Si and Ge, which are 14.7 and 4.15 meV, respectively. The linear in-

terpolation results in an estimate of 13.54 meV for the FE dissociation energy in the $x=0.11$ alloy.

A similar analysis has been applied to the $x=0.067$ sample, C021-3. As shown in Fig. 7, compared to sample C077 the luminescence from sample C021-3 is shifted to higher energy by 15.5 meV. This implies a band-gap decrease of 25.9 meV for the $x=0.067$ alloy. This result and the result previously obtained for sample C077 are consistent with the alloy-composition measurements presented in Table I if a linear relationship between the alloy composition and change in band gap is assumed. The composition ratio between the two samples is 0.609 while the ratio of the measured band-gap shifts is 0.626.

To compare the Si and $\text{Si}_{1-x}\text{Ge}_x$ luminescence energies for the In-doped sample, C093, we note that samples C077 and C093 differ in composition by only about 1%. We therefore assume that the FE binding energies in the two samples are the same. This leads to the comparison schematically illustrated in Fig. 12. The gap energy for sample C093, 1129.14 meV, was determined by adding the assumed FE binding energy, 13.34 meV, to the FE

threshold energy, 1115.8 meV. This results in a measured band-gap shift of 40.2 meV for the $x=0.104$ alloy. The band-gap shifts and alloy-composition measurements are reasonably consistent, assuming a linear relationship between the alloy composition and change in band gap. The composition ratio between samples C077 and C093 is 0.920 while the ratio of measured band-gap shifts is 0.971. Samples C021-3 and C093 agree exactly — the composition ratio and the ratio of measured band-gap shifts are both 0.644.

C. Excitons bound to composition fluctuations

One feature in the luminescence spectrum of sample C077 remains to be discussed. At high temperatures (Fig. 3), the FE line assumes a shape characteristic of FE recombination in Si and is well described by Eq. (1), as previously discussed. The FE threshold energy obtained by fitting Eq. (1) is independent of temperature, as expected. However, at low temperatures this is no longer the case. Spectra taken at various temperatures below 6 K are shown in Fig. 13. We see that as the temperature decreases, the line shifts to lower energy and assumes a shape which is no longer characteristic of FE recombination.

These measurements of low-temperature FE luminescence suggest that a low-energy shoulder appears on the FE luminescence at low temperatures. This shoulder may be due to the recombination of excitons bound by only about 0.1 meV to a very shallow level. This interpretation is supported by the temperature-resolved spectra, which show that the shoulder has completely thermalized by 6 K. Above 6 K, Eq. (1) correctly describes the line shape, and the threshold energy is independent of temperature. This behavior is consistent with a binding energy of tenths of meV. Also, the pump-power dependence at 1.6 K (Fig. 14) shows that the FE to BE_p intensity ratio is independent of pump power, as expected for independent exciton-binding centers in the absence of saturation.

These features, and the fact that there is no known defect or impurity in Si which binds an exciton by only 0.1 meV, leads us to suggest that the new feature may be due to the recombination of excitons weakly bound to local fluctuations in the alloy composition (BE_F). The possibility of such a state was first pointed out by Baranovskii and Efros,¹⁶ who extended the bulk fluctuation theory of Alferov *et al.*¹² to include excitons. A line

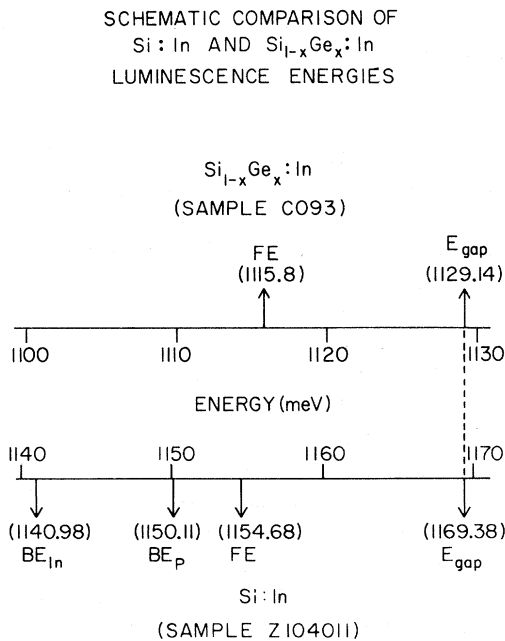


FIG. 12. Schematic line-position comparison between Si and $\text{Si}_{1-x}\text{Ge}_x$:In sample C093. This comparison is based on the assumption that the FE binding energy in sample C093 and sample C077 is identical. This fixes the alloy gap energy. The spectra are then compared by lining up the Si and $\text{Si}_{1-x}\text{Ge}_x$:In gap energies.

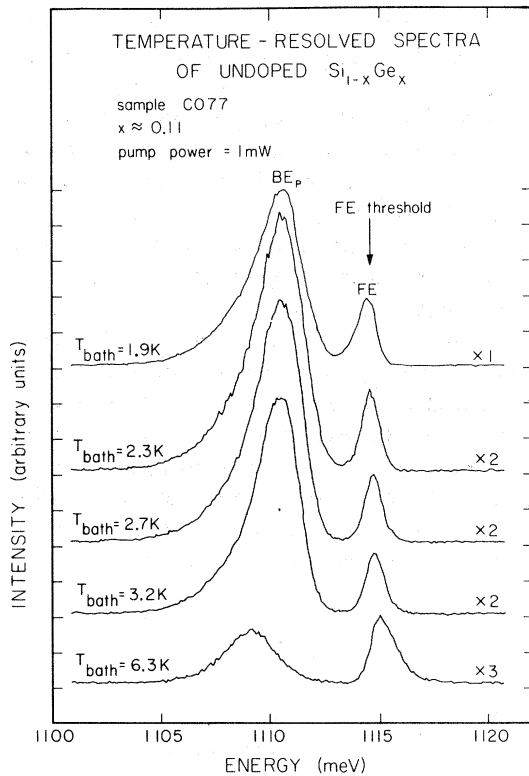


FIG. 13. Temperature-resolved spectra of undoped $\text{Si}_{1-x}\text{Ge}_x$ sample C077 at low temperatures. The scale factors (e.g., $\times 2$) give the relative intensity magnification. Note that the free-exciton line shifts and broadens as the temperature is decreased. For reference, the free-exciton threshold energy measured at high temperature is shown.

which may be due to fluctuation bound excitons has just recently been reported in $\text{GaAs}_{1-x}\text{P}_x$,¹⁷ and has characteristics which are similar to those of the line reported here.

One of the most important features of this model is the prediction that BE_F luminescence should have a very long lifetime. As indicated during the discussion of BE_P decay, the dominant decay mechanism for donor or acceptor BE's in Si is the Auger process. This results in observed decay rates which can be orders of magnitude larger than the radiative rates obtained from measured oscillator strengths.^{10,18} For instance, the BE_P radiative decay rate is estimated to be $5 \times 10^2 \text{ sec}^{-1}$, whereas the observed Auger decay rate is $3.7 \times 10^6 \text{ sec}^{-1}$.¹⁰ When an exciton is bound to a local composition fluctuation, however, the Auger

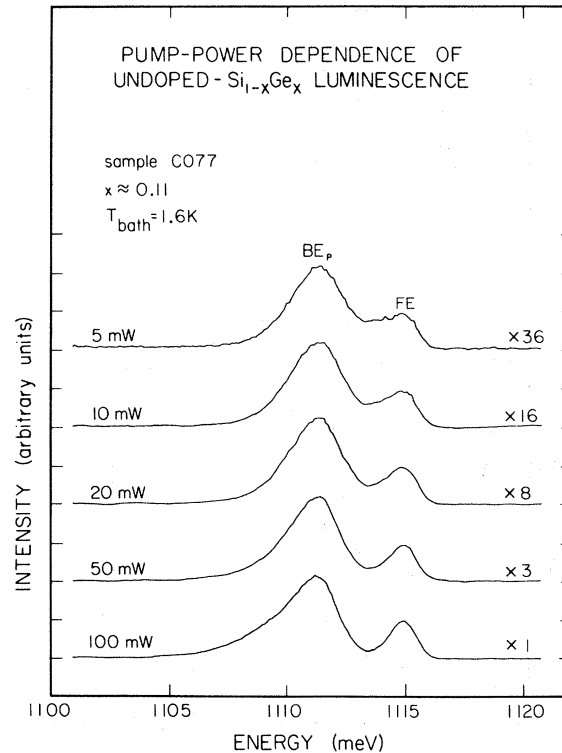


FIG. 14. Pump-power dependence of luminescence from undoped $\text{Si}_{1-x}\text{Ge}_x$ sample C077 at 1.6 K. The scale factors (e.g., $\times 36$) give the relative intensity magnification. Note that the BE_P -FE intensity ratio is independent of pump power.

process is not possible and long-lifetime luminescence is expected. Indeed, this was the case for the luminescence feature observed in $\text{GaAs}_{1-x}\text{P}_x$.¹⁶

Figure 15 presents the best low-temperature time-resolved spectra available for the $\text{Si}_{0.9}\text{Ge}_{0.1}$ alloy. Although the spectra are somewhat noisy, we see that the BE_F luminescence does not appear to have a particularly long lifetime compared to the BE_P luminescence line. This apparent discrepancy can be investigated by estimating the relevant decay times. These estimates show that in this case we are in a regime where the decays are capture limited,¹⁵ which explains why all components in the spectrum appear to decay with the same rate. Hence, while the low-temperature time-resolved spectra do not show long lifetimes for the BE_F luminescence, the data are not inconsistent with the model proposed above.

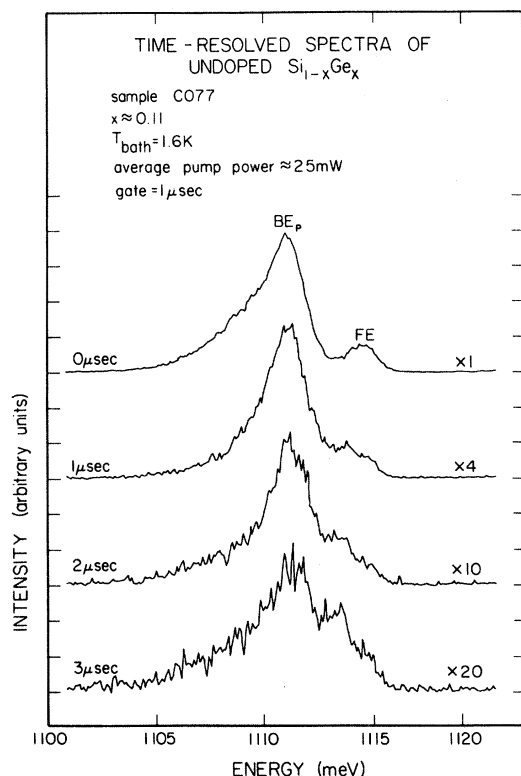


FIG. 15. Time-resolved spectra of undoped $\text{Si}_{1-x}\text{Ge}_x$ sample C077 at 1.6 K. The scale factors (e.g., $\times 4$) give the relative intensity magnification. Note that FE luminescence does not dominate the long-time spectrum.

VI. SUMMARY AND CONCLUSION

In this paper, we have presented the results of a study of the photoluminescence spectra of Si-rich $\text{Si}_{1-x}\text{Ge}_x$ alloy materials. Undoped and In-doped samples were considered in the range $0.067 \leq x$

≤ 0.11 . The luminescence features observed in the spectra were identified as free-exciton and bound-exciton luminescence. The free-exciton luminescence is described very accurately by the Si no-phonon free-exciton line shape, Eq. (1). As a result, a no-phonon free-exciton threshold energy was obtained for each sample.

In addition to this identification of the luminescence features, mechanisms for the observed bound-exciton—luminescence broadening were discussed. On the basis of this discussion, the Si-Ge luminescence energies were compared with those from Si, and values for the alloy band-gap shift and change in free-exciton binding energy were obtained. Finally, evidence was presented which may indicate that luminescence from excitons bound to local composition fluctuations is observed in the low-temperature luminescence spectra.

ACKNOWLEDGMENTS

The authors would like to thank R. Baron, J. Baukus, O. J. Marsh, and H. Kimura of Hughes Research Laboratories for growing and characterizing the Si-Ge alloy samples. Also, we have appreciated valuable discussions with Y. C. Chang, A. T. Hunter, and R. M. Feenstra. Finally, we acknowledge the financial support of the Office of Naval Research under Contract No. N00014-81-C-0285, and the National Sciences and Engineering Research Council of Canada.

¹A. Onton, *J. Lumin.* **7**, 95 (1973), and references therein.

²D. J. Wolford, R. E. Anderson, and B. G. Streetman, *J. Appl. Phys.* **48**, 2442 (1977), and references therein.

³Zh. I. Alferov, V. I. Amosov, D. Z. Garbuzov, Yu. V. Zhilyaev, S. G. Konnikov, P. S. Kop'ev, and V. G. Trofim, *Fiz. Tekh. Poluprovodn.* **6**, 1879 (1972) [*Sov. Phys.—Semicond.* **6**, 1620 (1973)], and references therein.

⁴A. T. Hunter, D. L. Smith, and T. C. McGill, *Appl. Phys. Lett.* **37**, 200 (1980), and references therein.

⁵See, for example, E. F. Gross, N. S. Sokolov, and A. N. Titkov, *Fiz. Tverd. Tela (Leningrad)* **14**, 2004 (1972) [*Sov. Phys.—Solid State* **14**, 1732 (1973)].

⁶R. Rentzsch and I. S. Shlimak, *Fiz. Tekh. Poluprovodn.*

12, 713 (1978) [*Sov. Phys.—Semicond.* **12**, 416 (1978)].

⁷C. Benoit à la Guillaume and M. Voos, *Phys. Rev. B* **10**, 4995 (1974).

⁸S. A. Lyon, D. L. Smith, and T. C. McGill, *Phys. Rev. Lett.* **41**, 56 (1978).

⁹R. B. Hammond, D. L. Smith, and T. C. McGill, *Phys. Rev. Lett.* **35**, 1535 (1975).

¹⁰W. Schmid, *Phys. Status Solidi B* **84**, 529 (1977).

¹¹S. A. Lyon, D. L. Smith, and T. C. McGill, *Phys. Rev. B* **17**, 2620 (1978).

¹²Zh. I. Alferov, E. L. Portnoi, and A. A. Rogazhev, *Fiz. Tekh. Poluprovodn.* **2**, 1194 (1968) [*Sov. Phys.—Semicond.* **2**, 1001 (1969)].

¹³J. P. Dismukes, L. Ekstrom, and R. J. Paff, *J. Phys.*

- Chem. 68, 3021 (1964).
- ¹⁴R. Braunstein, A. R. Moore, and F. Herman, Phys. Rev. 109, 695 (1958).
- ¹⁵G. S. Mitchard, Ph. D. thesis, California Institute of Technology, 1981 (unpublished).
- ¹⁶S. D. Baranovskii and A. L. Éfros, Fiz. Tekh. Poluprovdn. 12, 2233 (1978) [Sov. Phys.—Semicond. 12, 1328 (1978)].
- ¹⁷S. Lai and M. V. Klein, Phys. Rev. Lett. 44, 1087 (1980).
- ¹⁸G. C. Osbourn, S. A. Lyon, K. R. Elliott, D. L. Smith, and T. C. McGill, Solid State Electron. 21, 1339 (1978).